Molecular Cancer Therapeutics

Impact of Chemical-Induced Mutational Load Increase on Immune Checkpoint Therapy in Poorly Responsive Murine Tumors

Elizabeth A. Kuczynski[1], Janna Krueger[1], Annabelle Chow[1], Ping Xu[1], Shan Man[1], Yogi Sundaravadanam[2], Jessica K. Miller[2], Paul M. Krzyzanowski[2], and Robert S. Kerbel[1,3]

Abstract

A recurring historic finding in cancer drug development is encouraging antitumor effects observed in tumor-bearing mice that fail to translate into the clinic. An intriguing exception to this pattern is immune checkpoint therapy, as the sustained tumor regressions observed in subsets of cancer patients are rare in mice. Reasoning that this may be due in part to relatively low mutational loads of mouse tumors, we mutagenized transplantable mouse tumor cell lines EMT-6/P, B16F1, RENCA, CT26, and MC38 *in vitro* with methylnitro-nitrosoguanidine (MNNG) or ethylmethane sulfonate (EMS) and tested their responsiveness to PD-L1 blockade. Exome sequencing confirmed an increase in somatic mutations by mutagen treatment, an effect mimicked in EMT-6 variants chronically exposed *in vivo* to cisplatin or cyclophosphamide. Certain mutagenized variants of B16F1, EMT-6/P, CT26, and MC38 (but not RENCA) were more immunogenic than their parents, yet anti-PD-L1 sensitization developed only in some EMT-6/P and B16F1 variants. Treatment response patterns corresponded with changes in immune cell infiltration and especially increases in $CD8^+$ T cells. Chronically cisplatin-exposed EMT-6 variants were also more responsive to anti-PD-L1 therapy. Although tumor PD-L1 expression was upregulated in *in vivo* chemotherapy-exposed variants, PD-L1 expression levels were not consistently associated with anti-PD-L1 treatment activity across mutagenized or chemotherapy-exposed variants. In summary, mutagenized and more immunogenic mouse tumors were not universally sensitized to PD-L1 blockade. Chemically mutagenized variants may be useful to evaluate the impact of immunologically "hot" or "cold" tumors with a high mutational load, to which certain chemotherapy agents may contribute, on immunotherapy outcomes. *Mol Cancer Ther; 17(4); 869–82. ©2018 AACR.*

Introduction

Immune checkpoint inhibitors are a relatively new and successful therapeutic modality causing potent responses and prolonged survival times in patient subsets of certain malignancies. Two of the most important immune checkpoints are CTLA-4 that restricts initiation of T-cell responses in lymph nodes, and programmed death receptor 1 (PD-1)/PD-L1 that downregulates the activation and proliferation of antigen-specific T cells in tumors and peripheral tissues (1). Therapeutic antibodies against CTLA-4 and PD-1/PD-L1 therefore relieve immunosuppression and unmask antitumor effector T-cell responses.

It is emerging that cancer types that are most responsive to checkpoint inhibitors often have a high mutational load (2, 3). The reason is that such tumors have a greater likelihood of generating neoantigens that may be recognized by $CD4^+$ and $CD8^+$ T cells, thereby providing the necessary preexisting antitumor immunity. These cancers include melanoma and NSCLC that have on average the highest rate of nonsynonymous mutations due to mutagenic UV radiation and the carcinogens in tobacco, respectively, which drive their pathogenesis (2, 3). More prolonged and durable treatment benefit has also been observed in the subsets of patients with higher neoantigen and nonsynonymous mutational burden (4–7) or in patients with acquired or genetically predisposed mismatch repair (MMR) deficiency (8, 9). These genetic biomarkers are becoming crucial for the selection of patients who are more likely to benefit from immune checkpoint inhibition, as evidenced by the recent FDA approval of the PD-1 inhibitor pembrolizumab for any tumor type with MMR deficiency or microsatellite instability (10). Certain chemotherapy agents including temozolomide, nitrogen mustards, and platinum agents are also known carcinogens and mutagens (2, 11, 12). Although not currently well recognized, this may be an important consideration where patients are administered checkpoint inhibitors after receiving multiple lines of prior chemotherapy-containing regimens (13, 14).

In contrast to clinical results, immune checkpoint inhibitors as monotherapies often have no activity or merely delay growth in mouse tumor models—antitumor responses that clinically correspond to progressive disease (15, 16). One reason is that most syngeneic spontaneous and transplantable tumor models are weakly or nonimmunogenic (17). This is in part because such tumors likely underwent immune editing during their

[1]Biological Sciences Platform, Sunnybrook Research Institute, Toronto, Canada. [2]Ontario Institute for Cancer Research, Toronto, Canada. [3]Department of Medical Biophysics, University of Toronto, Toronto, Canada.

Note: Supplementary data for this article are available at Molecular Cancer Therapeutics Online (http://mct.aacrjournals.org/).

Corresponding Author: Robert S. Kerbel, Sunnybrook Research Institute 2075 Bayview Avenue, S-Wing, Room S217 Toronto, Ontario M4N3M5, Canada. Phone: 416-480-5711; Fax: 416-480-5884; E-mail: robert.kerbel@sri.utoronto.ca

doi: 10.1158/1535-7163.MCT-17-1091

development and were later propagated for efficient growth (18). A second related reason may be that mouse tumors have low mutational loads. Unlike their human tumor counterparts that may develop following decades of accumulating genetic damage, tumors arising spontaneously or from genetically engineered mice (GEMM) develop within months with reduced exposure to potential mutagenic or carcinogenic substances (19, 20). Mouse tumors grow rapidly *in vivo*, which further impairs the development of local inflammation and antitumor immunity.

The clinical relevance of mouse syngeneic tumor models is unclear. LLC and MAD109 lung cancers and B16 melanoma cell lines manifest high levels of local immunosuppression with low effector T-cell infiltration and immunotherapy resistance, directly contrasting with clinical observations in the corresponding cancers (17, 21, 22). Unlike MMR-proficient colorectal carcinomas (9), chemically induced MC38 and CT26 colon cancer cell lines are among the most immunogenic of syngeneic tumors and respond to some single-agent checkpoint inhibitors, but these models are highly variable with not all of treated tumors regressing within an experiment of genetically identical hosts (21, 23, 24). Recent correlations of mutational data with PD-1, PD-L1, and CTLA-4 inhibitor activity in several tumor models have not shown consistent trends (21, 24). It is presently unclear to what extent there is a cause-and-effect relationship between mouse tumor mutational load and immune checkpoint inhibitor responsiveness, as recently pointed out by Germano and colleagues (25).

We hypothesized that the limited immunogenicity of most conventional murine tumors and their limited responsiveness to immune checkpoint drugs could be altered by increasing their mutational load. One such method is by treatment of cells with chemicals including N-methyl-N′-nitro-N-nitrosoguanidine (MNNG) and ethylmethane sulfonate (EMS), which cause random point mutations in DNA (26). These chemicals generated highly immunogenic clones of various non- or poorly immunogenic tumor cell lines that were incapable of growing tumors in syngeneic hosts ("tum-" clones; refs. 27–29), yet grew progressively in irradiated mice (30). We therefore chemically mutagenized mouse tumor cell lines with MNNG and EMS and characterized several immune characteristics of these tumors. We also evaluated variants repeatedly exposed to potentially mutagenic cancer drugs, i.e., cisplatin or cyclophosphamide *in vivo* or *in vitro*. Finally, we evaluated the activity of PD-(L)1 inhibitors on parental and mutagenized or drug-treated tumors to directly evaluate the impact of mutational load increase and whether these mutagenized tumors might model checkpoint inhibitor–responsive patients.

Materials and Methods

Cell lines and mutagen treatment

RENCA and B16F1 were originally obtained from Dr. Isaiah J. Fidler (MD Anderson Cancer Center, Houston, TX). EMT-6/P (*P* = parental), EMT-6/CDDP, and EMT-6/CTX cells were originally obtained from Dr. Beverly Teicher (National Institutes of Health, Bethesda MD) and were derived following ten successive passages of EMT-6 tumors in mice repeatedly and transiently treated with potentially lethal high doses of cisplatin (EMT-6/CDDP), cyclophosphamide (EMT-6/CTX), or untreated (EMT-6/P; ref. 31). EMT-6/CTX2 was derived from an EMT-6/CTX tumor-bearing mouse resistant to two cycles of three treatments of 100 mg/kg CTX followed by a two week treatment break a (plus 150 mg/kg induction dose). EMT-6/P-2CDDP cells were previously generated following chronic *in vitro* exposure of EMT-6/P cells to increasing concentrations (up to 2 μmol/L) of cisplatin over 6 weeks (32). All cell lines were determined to be mycoplasma-free within 6 months of use at an external laboratory (Charles River) and internally using MycoAlert kit (Lonza).

Cells were treated with 1-methyl-3-nitro-1-nitrosoguanidine (MNNG) or ethylmethane sulfonate (EMS) *in vitro* to obtain multiclonal mutagenized variants of a higher mutational load. Protocols were adapted from prior studies (27, 29). Log-phase cells were resuspended at 1.2 million (MNNG) or 2.4 million (EMS) cells per 20-mL serum-free media. EMS/mL (0.5 μL) or 3 μg/mL MNNG or control treatment was added and incubated for 1 hour (MNNG) or 2 hours (EMS) at 37°C with gentle agitation. Treatment was inactivated in 10% sodium thiosulfate and cells washed twice then expanded uncloned *in vitro*. A total of 1,000 cells/well of 6-well plates were immediately seeded in triplicate to assess clonogenic survival. A second mutagenesis step was performed on recovered cells to generate MNNG+EMS+ (MNNG followed by EMS) or B16F1-EMS+EMS+ variants. One control variant per cell line was used for tumor studies.

In vivo studies

Tumors were grown in female Balb/c (EMT-6, RENCA, CT26) or C57Bl/6 mice (B16F1, MC38) aged 6–9 weeks. A total of 2×10^5 cells were implanted orthotopically in the right inguinal mammary fat pad for EMT-6 breast cancer, and subdermally for B16F1 melanoma cell lines. All other cell lines were inoculated subcutaneously (5×10^5 cells). A luciferase-tagged variant of RENCA used ($RENCA^{luc+}$), a kidney cancer line, is referred to as "RENCA". A total of 5×10^5 cells of EMT-6/P-Control, MNNG+, and MNNG+EMS+ variants were implanted orthotopically in female YFP-SCID mice (bred in-house). Animal protocols and experiments were carried out with the approval of the institutional Animal Care Committee in accordance to CCAC guidelines. Cell lines for *in vivo* studies were used between 1 and 3 passages after mutagen treatment.

Mice with established tumors (volumes 65–135 mm^3 depending on the model) were administered 100 μg i.p. of isotype control (rat IgG2b clone LTF-2) or anti-PD-L1 (10F.9G2 clone, both BioXCell) antibody on days 0, 3, and 7. Alternatively, 200 μg i.p. of rat anti-PD-1 (clone RMPI-14, BioXCell) or isotype control IgG2a (clone 2A3; both from BioXCell) were administered days 0, 2, 4, 6, 17, 19, 21, and 23. Chemotherapy-exposed EMT-6 variants were administered IgG2b or PD-L1 antibody in combination with vehicle or 6 mg/kg cisplatin (CDDP; Sigma) i.p. on days 1, 3, and 5.

Exome sequencing and bioinformatics

Qubit (Life Technologies) was used to quantify the gDNA and 3 μg was sheared to 150–200 bp fragments using a Covaris Sonicator (Covaris Inc). Illumina paired-end libraries were prepared using the Agilent Technologies SureSelect XT Library Prep Kit for Illumina sequencing (Agilent). From the purified library, 750 ng was used as input for 24-hour hybridization at 65°C to Agilent SureSelectXT Mouse All Exon (49.6 MB design) baits (Agilent Technologies). Targeted DNA was recovered using Dynabeads MyOne Streptavidin T1 (Life Technologies). Libraries were validated using the Agilent Bioanalyzer High Sensitivity DNA Kit (Agilent Technologies) and quantified on the QuantStudio3 Real-Time PCR Instrument (Thermo Fisher Scientific) according to the

standard manufacturer's protocols. Paired-end cluster generation and sequencing of 2 × 101 cycles was carried out for all eight libraries on the Illumina Hi-Seq 2500 platform (Illumina Inc.) in Rapid Run mode with four libraries per lane. Mutation profiles were analyzed using muTect 1.1.4 (33) and Strelka 1.0.13 (34) software.

Mutation profiles of EMT-6/P cell line samples were analyzed using muTect 1.1.4 (33) and Strelka 1.0.13 (34) software. SNPs were generated for mutagenized EMT-6/P cell line treated with EMS+, MNNG+, and MNNG+EMS+ using the parental cell line as a reference sample using both methods, and variant calls identified in both were intersected to increase specificity. These mutations were used for analyses of mutational loads. This method was repeated for MNNG+EMS+ mutagenized RENCA and its parental control, and EMT-6/P, EMT-6/CDDP, EMT-6/CTX, and EMT-6/CTX2 chemotherapy-exposed variants.

Flow cytometry analysis of tumor cells

Enzymatically digested tumor cells were stained with fixable viability stain 450, FcR blocked (both BD Pharmingen), and stained for surface markers using the following mAbs: CD45-APC-Cy7, CD3e-AF700, CD11b-PerCP (all from BD Biosciences), CD4-PE-Dazzle594, CD8a-PE-Cy7, CD25-PeCy5, Ly-6G/Ly-6C (Gr1)-BV650, PD-1-FITC, PD-L1-PE (all Biolegend). The gating strategy is shown in Supplementary Fig. S1. Tumor cells were harvested following *in vitro* culture and stained with PE-conjugated PD-L1 or rat isotype (Biolegend) and DAPI (Invitrogen) for PD-L1 expression. All samples were run on a BD LSRII flow cytometer and analyzed using FlowJo.

IHC

Formalin-fixed, paraffin embedded sections were stained using antibodies for Ki67 (clone D3B5, Cell Signaling Technology) or CD8a (clone GHH8, Dianova) with biotin-conjugated secondary antibodies (Jackson ImmunoResearch) and detected with Vector Elite HRP kit and DAB chromogen (Dako) with hematoxylin counterstain (Leica). Sections were visualized with a Carl Zeiss Axioplan 2 microscope and digital camera (Carl Zeiss Canada Inc.) and images acquired using AxioVision 3.0 software.

Statistical analysis

Differences in immune cell populations were evaluated by ANOVA followed by Kruskal–Wallis for multiple comparisons relative to the Isotype parental control group. The proportion of transition versus transversion mutations were analyzed by χ^2 test. *P* values less than 0.05 were considered statistically significant. The impact of cisplatin on EMT-6/CDDP and EMT-6/P-2CDDP tumor growth was evaluated by Tukey multiple comparisons. The mean and SEM are reported.

Results

Generation and growth of mutagenized mouse tumor variants

We first selected EMT-6/P breast cancer, RENCA kidney cancer, and B16F1 melanoma cells for mutagenesis treatment, which are examples of spontaneous (EMT-6 was originally derived from a hyperplastic nodule) and transplantable cell lines that form progressively growing poorly immunogenic tumors (17, 22). Cells were exposed *in vitro* to MNNG, EMS, or the two mutagens in sequence according to Fig. 1A. Cells were then expanded uncloned (29) to improve chances of generating clones cells capable of activating adaptive immunity while ensuring that variants would still be tumorigenic, ie. "tum+" (27). Thus, one "variant" line (consisting of heterogeneous cell populations) per mutagen treatment condition was generated for each parental cell line.

MNNG treatment in particular reduced clonogenic survival and led to longer recovery times of cell lines (Fig. 1B and C; Supplementary Fig. S2A–S2C), but once recovered, all variant cells grew well *in vitro* (Supplementary Fig. S2D and S2E). Only B16F1-EMS+EMS+ cells had a clonogenic survival advantage (Fig. 1C). Mutagenized variants remained morphologically similar to parental cells with the exception being MNNG-exposed B16F1, which in addition to some size and shape changes, lost their black pigment phenotype (Supplementary Fig. S2F–S2H).

Increased mutational load of mutagenized variants

We performed exome sequencing on EMT-6/P-mutagenized variant cells to assess their mutational loads. To capture induced somatic mutations including those in rare subpopulations, we used OnTarget calling and directly compared mutagenized variants to their parental cells. Mutagen treatment led to genetic mutations consisting primarily of "passenger" mutations [93%–96% of single nucleotide polymorphisms (SNP)] that represent the predominant source of neoepitopes recognized by T cells (ref. 35; Supplementary Tables S1 and S2). All classes of point mutations were represented, with EMS associated with preferential C→T transitions consistent with the effects of alkylating agents on DNA (Fig. 1C; ref. 26). MNNG produced a significantly higher proportion of transversions than transitions (Fig. 1D; $\chi^2 P < 0.0001$), which tend to be more deleterious on amino acid sequences. Transversions were recently associated with clinical benefit in pembrolizumab (anti-PD-1)-treated NSCLC patients (4).

Importantly, MNNG+ variant cells had a higher number of induced mutations (mutational load) than EMS+ cells, with 249 new detected SNPs, insertions, and deletions (Indels) in MNNG+ versus 32 in EMS+ cells (Fig. 1E). Moreover sequential mutagen treatment (MNNG+EMS+) had a cumulative effect resulting in 389 new mutations, a high proportion of which were shared by its MNNG+ precursor (Fig. 1F and G). Functional annotation of SNPs revealed gene clusters with low enrichment scores (maximum of 2.38), potentially reflecting the randomness of genetic alterations (Supplementary Table S3). MNNG+EMS+ variant gained mutations in 7 genes associated with DNA recombination (enrichment score 0.55) or DNA repair (enrichment score 0.20), altered pathways that may potentiate response to checkpoint blockade (8, 9). Specifically, mutations in Brca2, Spidr, and Smg1 were silent mutations. However, Mcm7 and Spidr downstream and intron variants, respectively, and Mdc1 and Nuggc missense mutations may have functional consequences. Taken together, treatment with MNNG or EMS alone or in sequence differentially increased the number of somatic mutations in tumor cells.

Growth of mutagenized variants in mice

We next assessed the immunogenicity of mutagenized variants *in vivo* based on their growth proficiency. All variants were tumorigenic in syngeneic mice (Fig. 2A–C) but for 2 of 3 cell lines, MNNG-mutagenized (and to a lesser degree MNNG+EMS+) variants were slower growing than parental controls (mean tumor growth inhibition 93% in EMT-6/P-MNNG+ and 65% in B16F1-MNNG+; Fig. 2A and B; Supplementary Table S4; Supplementary Fig. S3A). These reduced growth characteristics were

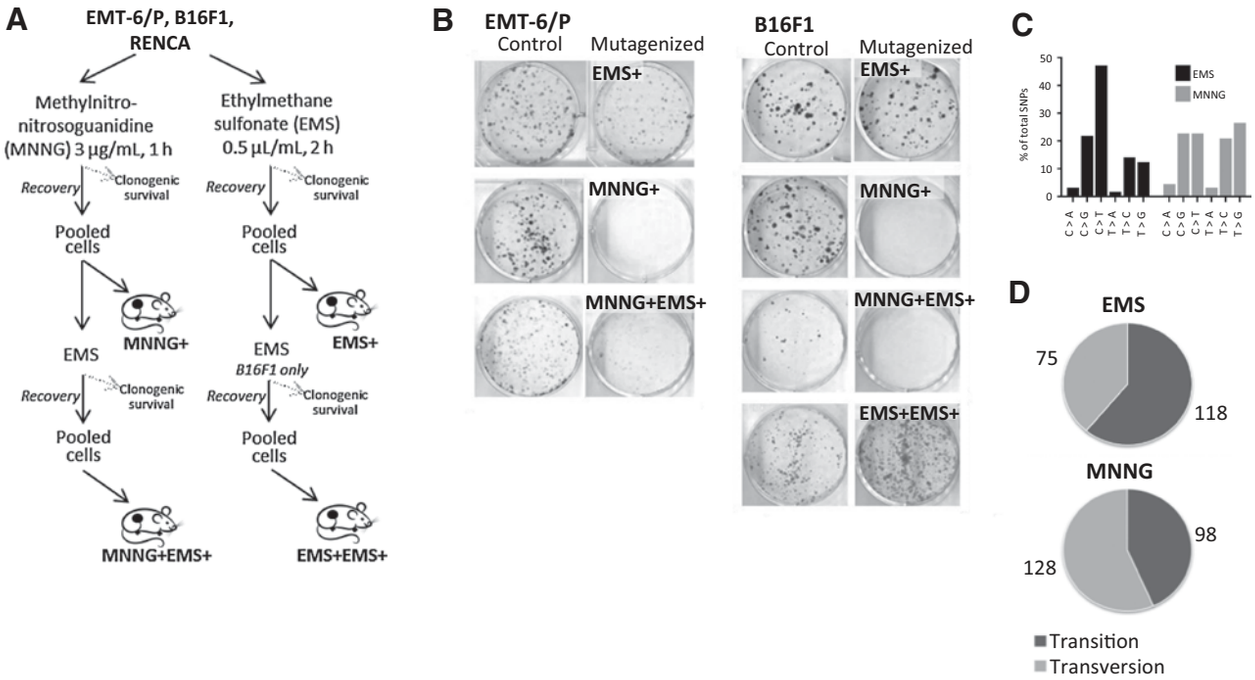

E

Mutation Type	EMS+	MNNG+	MNNG+ EMS+
3′ UTR variant	2	5	17
5′ UTR premature start codon gain variant			2
5′ UTR variant	2	5	6
Downstream gene variant		3	10
Frameshift variant			8
Inframe deletion	3	1	
Inframe insertion	1		
Intergenic region	4	10	17
Intron variant	9	52	78
Missense variant	5	110	149
Non coding exon variant		1	1
Splice donor variant		8	1
Splice region variant	1	4	18
Stop gained		3	4
Stop lost		1	1
Synonymous variant	5	38	67
Upstream gene variant		8	10
Total	**32**	**249**	**389**

Summary	EMS+	MNNG+	MNNG+ EMS+
SNPs	15	228	340
Indels	17	21	49
Total	**32**	**249**	**389**

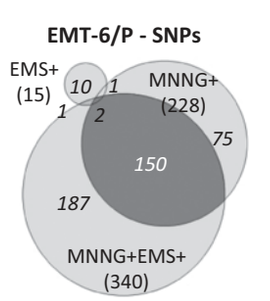

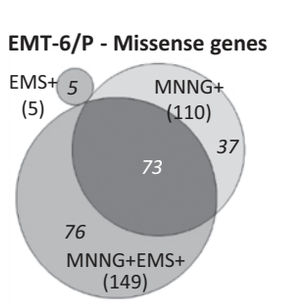

Figure 1.

Generation of mutagenized variants of murine tumor cell lines with increased mutational load. **A,** Protocol by which mouse cancer cell lines were mutagenized *in vitro* with single or sequential treatment of methylnitro-nitrosoguanidine (MNNG) or ethylmethane sulfonate (EMS). Surviving cell populations were implanted into mice for tumor studies. **B,** Clonogenic survival of control (parental) and mutagenized EMT-6/P and B16F1 cell lines seeded immediately following mutagen treatment. Each mutagenized variant (right) is shown next to its matched control (left). **C,** Mutational signature for all detected SNPs produced by EMS or MNNG treatment as determined by exome sequencing. EMS point mutations were pooled from those acquired by EMS+ variant and by EMS mutagen treatment of MNNG+ variant, totaling 193 mutations for EMS and 226 for MNNG. **D,** Proportion of transition versus transversion mutations induced by EMS or MNNG. MNNG treatment resulted in a significantly higher proportion of transversion mutations than EMS (χ^2 test statistic = 13.17, $P < 0.0001$). **E,** Summary of somatic mutations detected by exome sequencing of EMT-6/P variants harvested from culture. Mutations are those acquired by mutagenesis relative to parental control cells. **F,** Total (in brackets) and shared quantity of de novo acquired SNPs and missense genes (**G**) in EMS+, MNNG+, and MNNG+EMS+ EMT-6/P mutagenized variants.

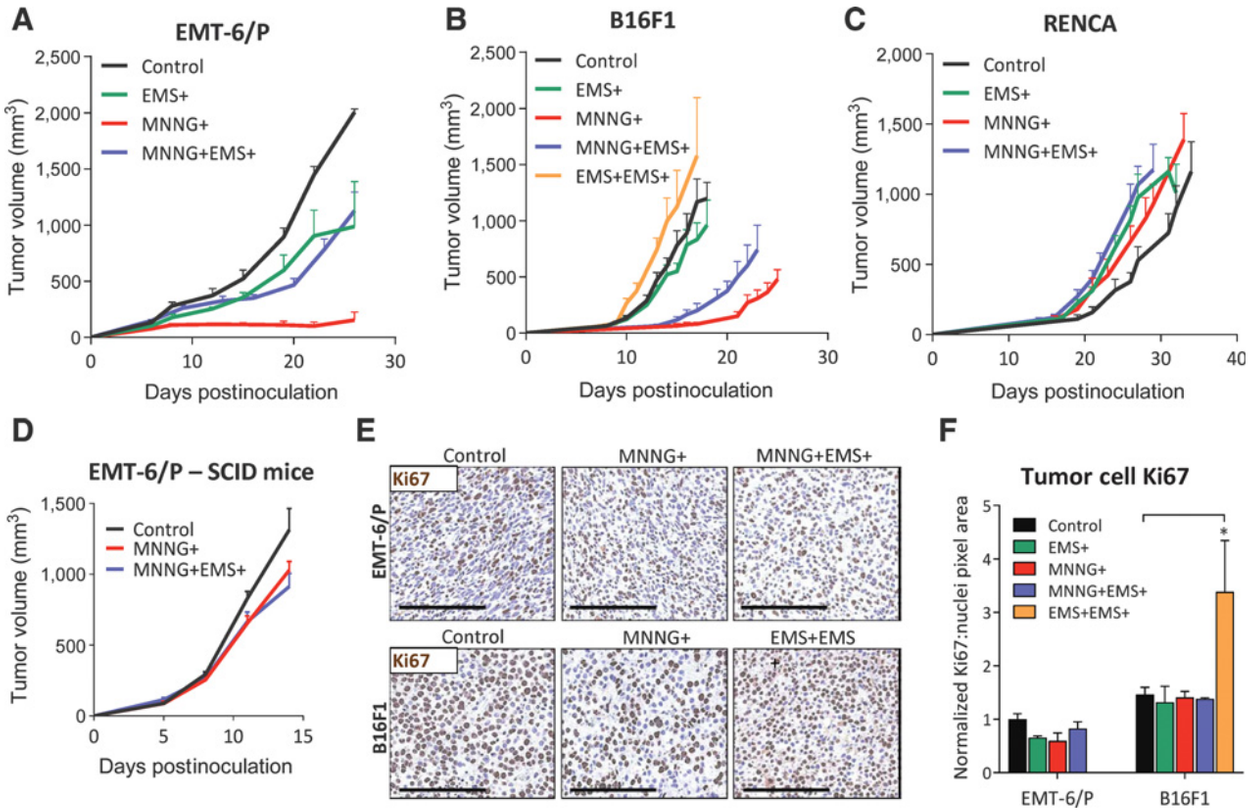

Figure 2.

Variable *in vivo* growth patterns of mutagenized variants. **A,** Growth of orthotopic (intramammary fat pad) EMT-6/P breast tumor variants in immunocompetent Balb/c mice ($n = 5$). Average tumor volume is shown. Growth of subdermal B16F1 variants ($n = 6$–7; **B**), and subcutaneous RENCA variant tumors ($n = 6$–7; **C**) in C57Bl/6 or Balb/c mice, respectively. **D,** Growth of orthotopic EMT-6/P mutagenized variants in immunocompromised SCID mice ($n = 5$) showing robust growth. Mice in **A–D** had been treated with 3 intraperitoneal doses of 100 μg IgG2b isotype control once tumors became established in therapy studies (see Fig. 3). **E,** IHC staining for mouse Ki67 (brown) in tumors grown in syngeneic mice. Nuclei were counterstained with hematoxylin (blue). Scale bar = 200 μm. **F,** Quantification of tumor cell Ki67 showing a statistically significant increase ($P = 0.012$) in Ki67 signal in B16F1-EMS+EMS+ tumors relative to B16F1-Control tumors. Data represents the mean value obtained from 4–5 tumors [except EMT-6/P-MNNG+ ($n = 2$) and B16F1-EMS+ ($n = 3$) due to limited viable tumor tissue] normalized to the parental control for EMT-6/P. Error bars, SEM.

likely to be primarily immunologic because EMT-6/P-MNNG+ and MNNG+EMS+ variants grew progressively in SCID mice lacking functional T cells (Fig. 2D; although EMT-6/P-MNNG+EMS+ doubling time was significantly shorter in SCIDs; *t* test versus Control $P = 0.020$ in SCID, $P = 0.061$ in Balb/c; Supplementary Table S4). Furthermore, the intrinsic proliferation rate of EMT-6/P or B16F1 mutagenized variant tumor cells based on IHC for Ki67 was not significantly changed compared with their parental controls in syngeneic hosts ($P > 0.05$; Fig. 2E and F). EMS+ tumors typically progressed similar to controls (Fig. 2A–C), but interestingly, B16F1-EMS+EMS+ tumors grew more rapidly *in vivo* which corresponded to a significant increase in tumor cell proliferation ($P < 0.05$; Fig. 2B, E, and F).

All mutagenized variants of RENCA progressed at least as rapidly as the parent *in vivo* (Fig. 2C; Supplementary Table S4). This was not due to a lack of mutational load increase as confirmed by exome sequencing; however, the magnitude of increase in RENCA-MNNG+EMS+ was 5.6-fold lower than that observed in the EMT-6/P-MNNG+EMS+ variant relative to their respective controls (Supplementary Fig. S3B). Thus, in EMT-6/P and B16F1, but not RENCA cell lines, tumor immunogenicity (growth proficiency) was concordant with the stronger mutagenic effect of MNNG over EMS (Fig. 1E). Sequentially mutagenized MNNG+EMS+ variants were exceptional in that a second exposure with EMS partially restored the growth of MNNG+ variant.

Response of chemically mutagenized variants to PD-(L)1 blockade

Improved clinical outcomes with immune checkpoint inhibitors have been assessed to be associated with a higher mutational load in multiple tumor settings (4–9); therefore, we evaluated whether mutagenized tumors showed evidence of increased anti-PD-L1 (10F.9G2 clone) treatment activity. Parental controls of B16F1 and RENCA were highly refractory to PD-L1 blockade while EMT-6/P exhibited antitumor responses in a subset of mice (Fig. 3A, E and I; Supplementary Table S4). Akin to clinical observations (4–9), PD-L1 inhibition was potentiated in some mutagenized tumor variants: potent tumor regressions occurred in 5 of 5 treated EMT-6/P-MNNG+EMS+ tumors (vs. 1/5 control tumors) and delayed growth of B16F1-MNNG+EMS+ tumors (Fig. 3D and G). EMT-6/P-EMS+ was marginally sensitized to anti-PD-L1 treatment

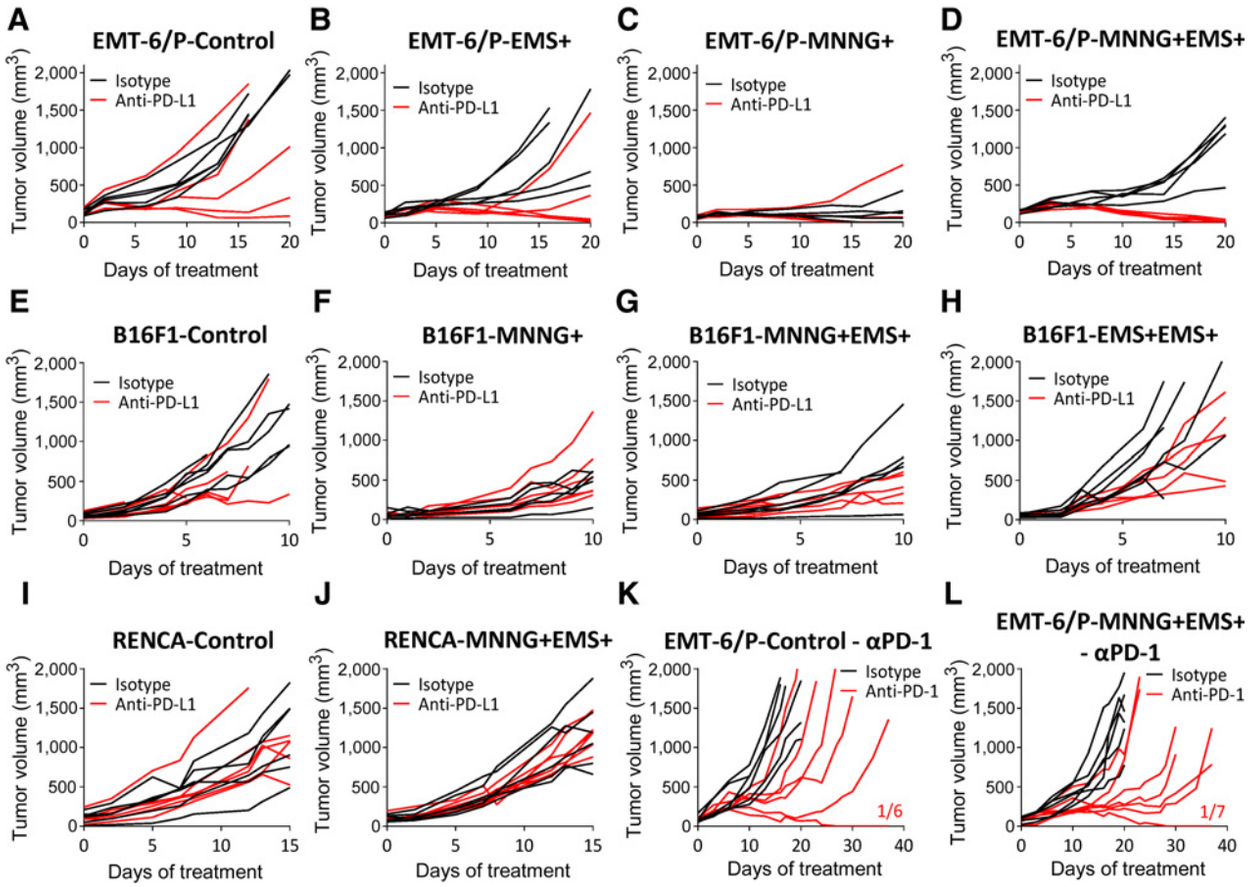

Figure 3.

Response of mutagenized tumor variants to PD-L1 and PD-1 immune checkpoint antibody treatment. Mice with established tumors were randomized to 3 × 100 μg i.p. anti-PD-L1 rat monoclonal antibody (anti-PD-L1) or isotype IgG2b control (Isotype) treatment for days 0, 3, and 7. Day 0 represents when treatment was initiated. Plots of individual mouse tumor volumes showing variable responses to anti-PD-L1 treatment are shown for Control, EMS+, MNNG+, and MNNG+EMS+ variants of EMT-6/P ($n = 5$) (**A–D**), and Control, MNNG+, MNNG+EMS+ and EMS+EMS+ variants of B16F1 ($n = 6$–7; **E–H**). **I** and **J,** Control and MNNG+EMS+ RENCA tumor variants during anti-PD-L1 treatment ($n = 6$–7). **K** and **L,** Mice with established EMT-6/P-Control (**K**) or EMT-6/P-MNNG+EMS+ tumors (**L**) were randomized to 200 μg i.p. anti-PD-1 rat monoclonal antibody (anti-PD-1) or isotype IgG2a control (isotype) treatment for days 0, 2, 4, 6, 17, 19, 21, and 23. The fraction of anti-PD-1–treated tumor-free mice is indicated.

(3/5 tumors regressing; Fig. 3B), whereas comparatively, the B16F1 model was refractory since two exposures of cells to EMS (B16F1-EMS+EMS+) were necessary to achieve growth delay (Fig. 3H; Supplementary Fig. S4A).

The above data suggested an exposure–response relationship between *in vitro* mutagen treatment and immune checkpoint inhibitor responsiveness; however, there were exclusions and limitations to this rule. First, neither of the inherently immunogenic B16F1-MNNG+ and EMT-6/P-MNNG+ variants (Fig. 2A and B) were more treatment-responsive (Fig. 3C and F). The apparent improvement in EMT-6/P-MNNG+ tumors was obscured by spontaneous regressions during isotype control treatment (Fig. 3C). Second, all mutagenized RENCA tumor variants remained resistant to PD-L1 blockade (Fig. 3I and J). Third, the added benefit from an alternate checkpoint inhibitor, a PD-1 antibody, was less durable (minor prolongation of tumor growth control) than that of the PD-L1 antibody (Fig. 3K–L). Finally, anti-PD-L1 activity was critically dependent on a low tumor burden. All but one of large (400 mm^3) EMT-6/P-MNNG+EMS+ tumors were unresponsive to anti-PD-L1 treatment. Among small (130 mm^3) tumors, 2 of 8 mice were ultimately cured and demonstrated immunologic memory due to rejection of tumor rechallenge (on day 58; Supplementary Fig. S4B and S4C). Rapid growth within the first days of treatment also appeared to contribute to the variability in rates of small tumor regression (Fig. 2). Taken together, a minority of chemically mutagenized variants was sensitized to immune checkpoint therapy and this was not restricted to the slowest growing and immunogenic of variants.

Immune cell infiltration in mutagenized tumors

Higher somatic mutational load in cancer patients has been associated with increased tumor infiltration with cytotoxic T cells and fewer immunosuppressive cells (36, 37). We evaluated the immune cell profile of mutagenized and anti-PD-L1–treated tumors and indeed observed a shift in immune landscapes. An average 19.1-fold increase in $CD4^+$ helper T cells and 10.8-fold increase in $CD8^+$ cytotoxic T cells were observed in

EMT-6/P-MNNG+EMS+ tumors, with greater increases in EMT-6/P-MNNG+ tumors, altogether reinforcing their differential growth rates *in vivo* (Fig. 4A, 2A and D). $CD8^+$ T cells also increased 4.4-fold in B16F1-MNNG+EMS+ and 1.6-fold in B16F1-EMS+EMS+ isotype-treated tumors, although the results were not statistically significant ($P > 0.05$; Fig. 4B). Mutagenesis did not alter the immune cell profile of RENCA tumors which consisted almost entirely of tumor-associated macrophages (TAM) and myeloid-derived suppressor cells (MDSCs; Fig. 4C), coinciding with their poor immunogenicity and immunotherapy resistance (Fig. 2C, 3I and J). $CD8^+$ T cells increased relative to parental or mutagenized tumor isotype controls in most instances of anti-PD-L1 antibody activity, including EMT-6/P-MNNG+EMS+ ($P < 0.05$ vs. isotype-treated parental control by multiple comparisons, or vs. MNNG+EMS+ isotype control by *t* test; Fig. 4A), B16F1-MNNG+EMS+ ($P < 0.01$ vs. parental; $P < 0.01$ vs. MNNG+EMS+ isotype; Fig. 4B), and B16F1-EMS+EMS+ ($P = 0.059$ vs. parental; $P = 0.33$ vs. EMS+EMS+ isotype). Finally, significant ($P < 0.05$) reductions in TAMs were observed in EMT-6/P-MNNG+, anti-PD-L1 EMS+ and MNNG+EMS+ tumors corresponding with their lower tumor burden (Figs.3B–D and 4A).

Histologically, all EMT-6/P variant tumors were infiltrated with $CD8^+$ T cells, a phenotype of "preexisting immunity" associated with sensitivity to checkpoint blockade in patients (ref. 38; Fig. 4D). Densely packed lymphocytes, suggestive of a local immune response, also comprised the bulk of many regressing MNNG+ and MNNG+EMS+ tumors (Supplementary Fig. S5A). Parental RENCA and B16F1 were nearly devoid of $CD8^+$ T cells (Fig. 4E and F), an "immunologically ignorant" phenotype linked to therapy resistance (38). RENCA-MNNG+EMS+ tumors maintained this phenotype, but slightly enhanced $CD8^+$ T-cell infiltration was observed in B16F1-MNNG+ and MNNG+EMS+ tumors (Fig. 4E and F). Immunologic differences could not be explained by *in vitro* MHC-I expression (EMT-6/P H2-Kd^{high}, B16F1 H2-Kb^{low}, RENCA H2-Kd^{high}), which remained unchanged on mutagenized tumor cells (Supplementary Fig. S5B). Taken together, *in vivo* growth rates and anti-PD-L1 treatment responses in mutagenized tumors tended to correspond with immune cell infiltration patterns, supporting the concept that a pre-existing immunity and a higher mutational load are requirements for a favorable response to checkpoint blockade (38).

PD-1/PD-L1 expression patterns

Having generated tumor sublines with differential genetic and immune infiltrate characteristics, we correlated these features with PD-1/PD-L1 expression in the tumor microenvironment. EMT-6/P and B16F1 parental lines expressed low and moderate levels of PD-L1, respectively, that were induced *in vivo* (Fig. 4G) and reverted to baseline in culture (Supplementary Fig. S5C). Inducible PD-L1 may indicate local IFNγ-producing T cells (39), although expression levels were unaltered in mutagen-exposed tumor cells (Fig. 4G). RENCA constitutively expressed high PD-L1, potentially contributing to high local immunosuppression in this model (Figs. 4C and 5A; ref. 39). Changes in expression of PD-L1 on TAMs and MDSCs and PD-1 on $CD8^+$ T cells were variable and cell line dependent (Fig. 4H and I; Supplementary Fig. S5D and E). For example, PD-1 expression on $CD8^+$ T-cells significantly decreased ($P < 0.01$ by %PD-1+ cells) in MNNG+EMS+ versus parental EMT-6/P tumors, but a similar trend did not occur in other models (Supplementary Fig. 5E). PD-1/PD-L1 immune checkpoint expression was therefore not indicative of anti-PD-L1 treatment response (39) across mutagenized tumors.

Immunogenic mutagenized tumors and anti-PD-L1 response

The above data suggest that PD-L1 blockade activity corresponded with the degree to which mutagen treatment enhanced antitumor immunity (summarized in Fig. 5A). Furthermore, these changes were most impactful in the more immunogenic EMT-6/P cell line. We therefore reasoned that highly immunogenic cell lines are more likely to be therapy sensitized using this methodology. We tested this hypothesis on murine colorectal carcinoma cell lines CT26 and MC38— highly immunogenic, progressively growing syngeneic tumors with higher mutational loads than EMT-6, RENCA, and B16 melanoma. *In vivo*, subcutaneous MNNG+EMS+ tumor variants of CT26 and MC38 had similar kinetics as parental controls for the first week (Fig. 5B) after which tumors slowed or spontaneously regressed, implicating an immunologic response. Complete spontaneous tumor regressions occurred in 2 of 16 of CT26-MNNG+EMS+ and 5/14 MC38-MNNG+EMS+ tumors, with additional mice exhibiting stabilized tumor growth (lasting 7–20 days; Fig. 5B and C). All tumor-free mice rejected rechallenge with their respective mutagenized (CT26) or parental (MC38) variants. Parental CT26 and MC38 were respectively weakly or moderately responsive to PD-L1 antibody (Fig. 5D and F). Surprisingly, among progressing tumors randomized to PD-L1 antibody, antitumor activity was not greater (and perhaps lower in MC38-MNNG+EMS+) than in parental tumors (Fig. 5E and G). Thus, mutational load increase in highly immunogenic tumor variants did not guarantee PD-L1 antibody activity.

Chemotherapy-exposed variants and PD-L1 blockade

A side-effect of certain DNA-damaging chemotherapy agents is their ability to induce mutations in surviving tumor cells, thereby contributing to tumor progression and drug resistance. We evaluated the hypothesis that this could also enhance the efficacy of checkpoint blockade using tumor cells repeatedly exposed over long periods to cisplatin and cyclophosphamide. These agents are known to cause crosslinks and adducts in DNA (11). EMT-6/CDDP and EMT-6/CTX variants were generated by Teicher and colleagues by transiently treating EMT-6 tumor-bearing mice with a lethal dose of cisplatin or cyclophosphamide, then removing the tumors and repeating exposures for 10 passages in consecutive new hosts (refs. 31, 32; Fig. 6A). These mimic a clinical chemotherapy regimen of multiple treatment cycles – albeit not using lethal dosing and short term exposures.

By exome sequencing, EMT-6/CDDP cells had striking more detected somatic mutations (2292 SNPs and 459 Indels) relative to the parental line, as did EMT-6/CTX cells (1014 SNPs, 403 Indels; Figs. 1C and 6B). A new variant (EMT-6/CTX2) derived after *in vivo* treatment of an EMT-6/CTX tumor with two cycles of MTD cyclophosphamide (Xu and Chow, unpublished results; Fig. 6A) had a further increase to 1,234 SNPs and 424 Indels (Fig. 6C). The mutational signature of CTX and CDDP had similarities with that of MNNG, including a high frequency of transversions (Supplementary Fig. S6). Similar to MNNG+EMS+ mutagenized tumors (Fig. 3), EMT-6/CDDP tumors were more responsive to anti-PD-L1 treatment compared with EMT-6/P controls (Fig. 6D and E).

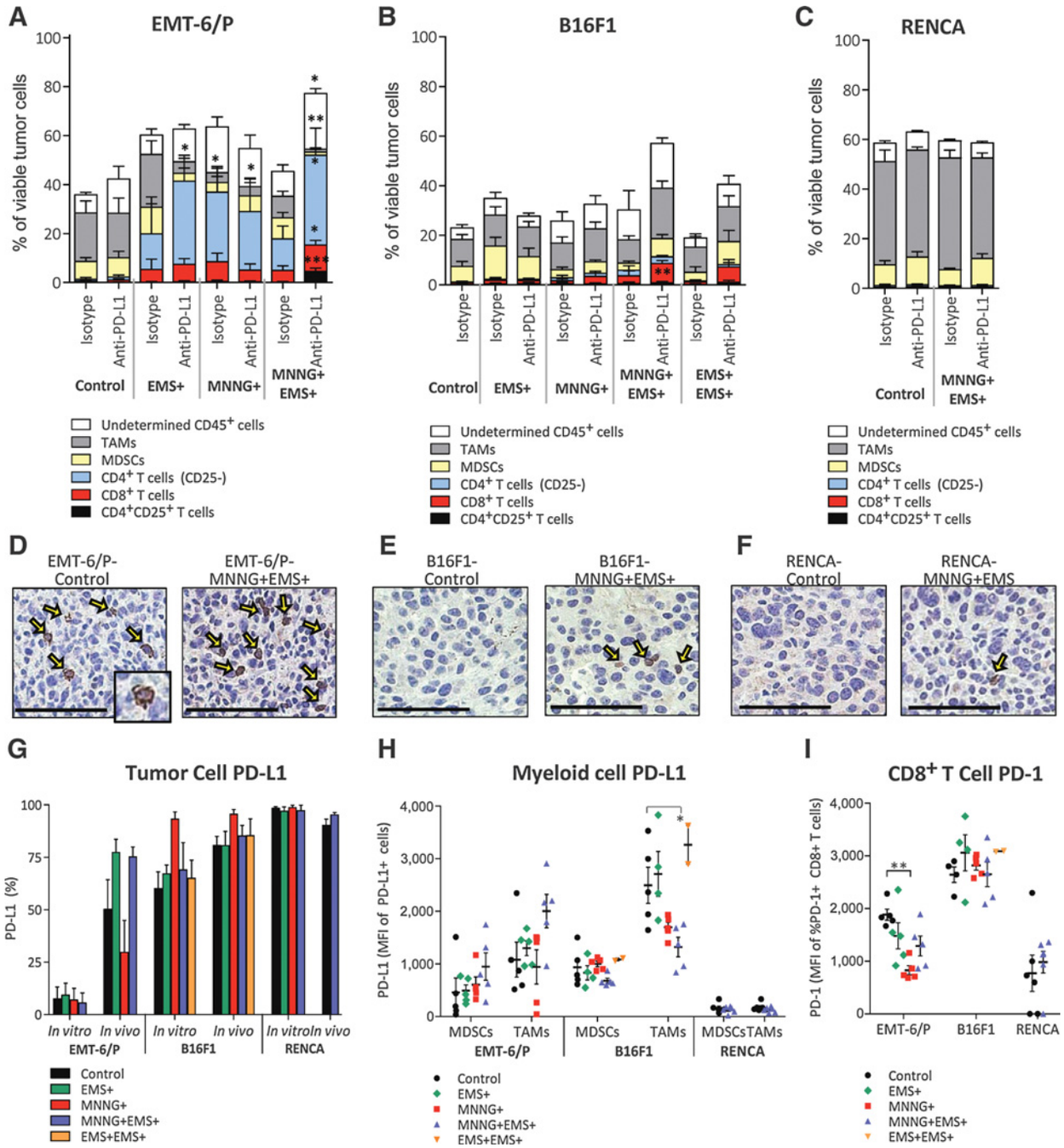

Figure 4.

Immune cell profiles and infiltration patterns of mutagenized tumors. **A,** The immune cell makeup of dissociated tumors was determined and expressed as the percent of myeloid and T lymphocyte CD45$^+$ subpopulations out of total viable tumor cells. Immune cell populations in isotype and anti-PD-L1–treated EMT-6/P, B16F1 (**B**) and RENCA mutagenized tumor variants (**C**). CD8$^+$ T cells are defined as CD45$^+$CD3$^+$CD4$^-$CD8$^+$, CD4$^+$ T cells as CD45$^+$CD3$^+$CD4$^+$CD8$^-$ (CD25$^+$ for regulatory T cells or CD25$^-$ for helper T cells), TAMs as CD45$^+$CD3$^-$CD11b$^+$Gr1$^-$ and MDSCs as CD45$^+$CD11b$^+$Gr1$^+$ (Ly6C/Ly6G). Note anti-PD-L1 B16F1-control tumor samples were unavailable due to mice prematurely reaching tumor ulceration endpoint. **D,** CD8$^+$ T-cell infiltration of tumors determined by IHC for CD8 antigen (brown) in EMT-6/P, B16F1 (**E**) and RENCA (**F**) control and mutagenized tumors. Yellow arrows indicate CD8$^+$ T cells (magnified in inset). Sections were counterstained with hematoxylin (blue). **G,** Parental and mutagenized tumor cell expression of PD-L1 assessed *in vitro* and *in vivo* on CD45$^-$ tumor cells. B16F1-MNNG+ PD-L1 $P = 0.087$ *in vitro* by multiple comparisons and $P = 0.087$ *in vivo*. EMT-6/P *in vivo* PD-L1 expression ANOVA $P = 0.021$. **H,** PD-L1 expression on MDSCs and TAMs in mutagenized tumor variants expressed as the MFI of %PD-L1$^+$ cells. A significant decrease in TAM PD-L1 expression in B16F1-MNNG+EMS+ tumors was observed relative to parental controls ($P = 0.022$). **I,** PD-1 expression on CD8+ T cells, expressed as the MFI of %PD-1$^+$ cells, in isotype-treated mutagenized tumor variants. CD8$^+$ T-cell PD-1 significantly decreased in EMT-6/P-MNNG+ tumors ($P = 0.0013$) and approached significance for EMT-6/P-MNNG+EMS+ tumors ($P = 0.063$). *, $P < 0.05$; **, $P < 0.01$; ***, $P < 0.001$. Scale bar = 100 μm. Error bars, SEM. TAMs, tumor-associated macrophages; MDSCs, myeloid-derived suppressor cells; MFI, mean fluorescence intensity.

A

	EMT-6/P-MNNG+EMS+		B16F1-MNNG+EMS+		RENCA-MNNG+EMS+	
Mutational load increase †	High		ND		Low	
Growth rate reduction †	Low		High		None	
Anti-PD-L1 response †	High		Low		None	
Treatment	***Iso***	***PD-L1***	***Iso***	***PD-L1***	***Iso***	***PD-L1***
$CD45^+$ total immune cells ‡	=	+	=	+	=	=
$CD4^+$ T cells (CD25-) ‡	+ +	+ +	+ +	+ +	=	=
$CD4^+CD25^+$ T cells ‡	+	+ +	+	=	=	=
$CD8^+$ T cells‡	+ +	+ +	+	+ +	=	=
MDSCs‡	=	- -	-	-	=	=
TAMs‡	-	- -	=	=	=	=
PD-L1 on MDSCs §	+	*n/a*	=	*n/a*	=	*n/a*
PD-L1 on TAMs §	=	*n/a*	=	*n/a*	=	*n/a*
PD-1 of CD8+ T cells §δ	-	- -	=	+	+	+

% of Control (Isotype)	
< 20 %	- -
20-49 %	-
50-150 %	=
151-300 %	+
> 300 %	+ +

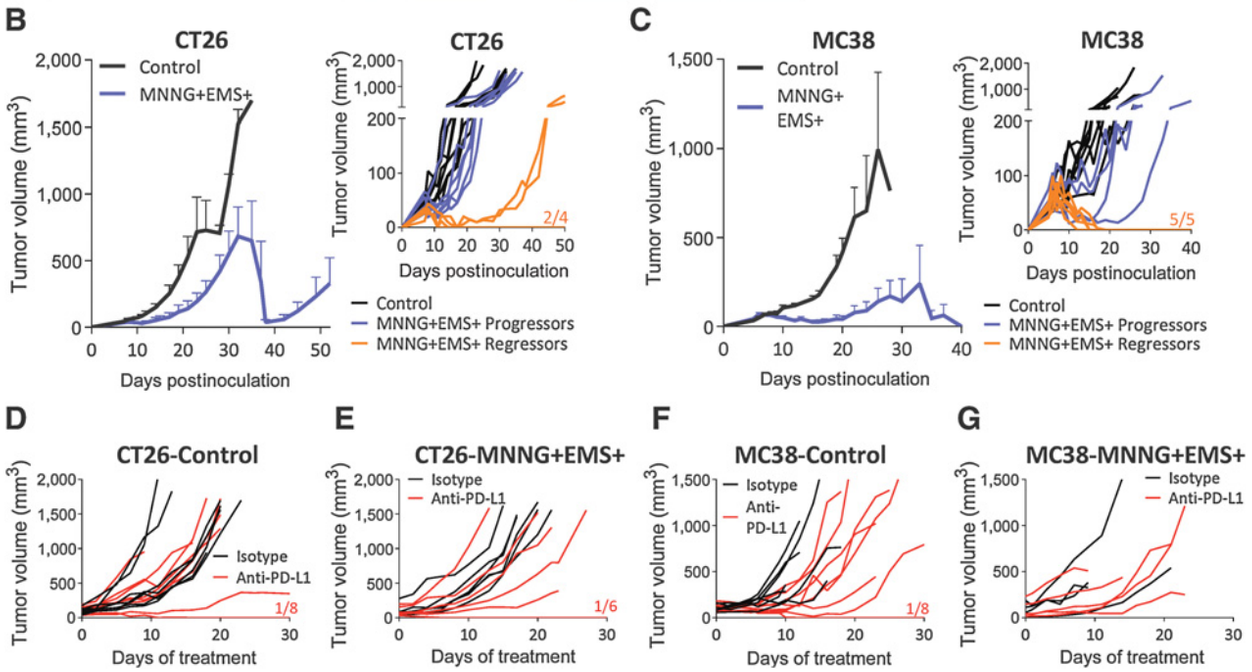

Figure 5.

Heterogeneous effects of mutagenesis on tumor immunogenicity and anti-PD-L1 responses. **A,** Summary of growth rate, treatment sensitivity, and immunologic changes in MNNG+EMS+ isotype (Iso) and anti-PD-L1 (PD-L1) mutagenized tumors. The mean change as a proportion of the parental isotype–treated control for each cell line (set at 100%) is shown according to the legend. †, Relative, qualitative changes relative to the parental control. ‡, Proportion out of total viable tumor cells. §, PD-1 or PD-L1 expression by MFI of % positive cells. δ, Numerical data on PD-1 expression from anti-PD-L1 tumors not shown. ND, not determined; n/a, not applicable due to potential detection antibody blockage by therapeutic antibody (both anti-PD-L1 clone 10F.9G2). **B,** *In vivo* growth of subcutaneous CT26 tumors ($n = 7$) and its MNNG+EMS+ mutagenized variant ($n = 10$). Mean tumor volumes (left) showing growth delay of MNNG+EMS+ mutagenized tumors which consisted of progressing tumors ("progressors"; $n = 6$ isotype treated tumors for therapeutic study) and spontaneously regressing tumors ("regressors"; $n = 4$ untreated tumors). Individual tumor volumes are shown at right. **C,** Growth of MC38 tumors ($n = 7$) and its MNNG+EMS+ mutagenized variant ($n = 9$). Mean (left) and individual (right) plots of tumor volumes showing mixture of progressors ($n = 4$) and spontaneous regressors ($n = 5$) in the MC38-MNNG+EMS+ tumor variant. **D,** Response of CT26-Control and (progressor) CT26-MNNG+EMS+ variants (**E**) during isotype control or anti-PD-L1 antibody treatment given 3 × 100 μg i.p. days 0, 3, and 7. Day 0 represents when treatment was initiated. **F,** Tumor growth of MC38-Control and progressor MC38-MNNG+EMS+ variants (**G**) during isotype and PD-L1 antibody treatment. The fraction of tumor-free mice is shown (**B–F**). MFI, mean fluorescence intensity; TAMs, tumor-associated macrophages; MDSCs, myeloid-derived suppressor cells.

A similar result was observed using another variant chronically exposed *in vitro* to escalating concentrations of CDDP (EMT-6/P-2CDDP; Fig. 6F; ref. 32). In contrast, many EMT-6/CTX tumors were not therapy-responsive (Fig. 6F). Treatment response patterns were not predicted by tumor PD-L1 expression, though interestingly, *in vivo* (but not *in vitro*) chemotherapy-exposed EMT-6 variants constitutively upregulated PD-L1 ($P < 0.05$; Fig. 6H). A rational therapeutic strategy might be to combine PD-L1 antibody with

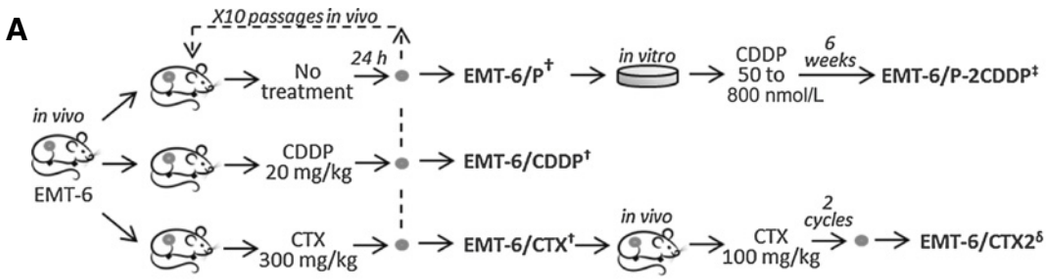

B

Mutation Type	EMT-6/CDDP	EMT-6/CTX	EMT-6/CTX2
3′ UTR variant	80	64	77
5′ UTR premature start codon gain variant	2	3	2
5′ UTR variant	26	15	15
Disruptive inframe deletion	3	2	2
Disruptive inframe insertion	1		
Downstream gene variant	48	37	38
Frameshift variant	86	49	54
Frameshift variant+start lost	1		
Inframe deletion	2	3	4
Inframe insertion		1	1
Intergenic region	72	48	55
Intron variant	645	405	445
Missense variant	1136	487	601
Non coding exon variant	15	8	9
Splice acceptor variant	23	8	9
Splice donor variant	17	4	4
Splice region variant	134	77	87
Start lost	3	1	
Stop gained	37	24	
Stop lost	2		
Stop retained variant	1		27
Synonymous variant	358	140	177
Upstream gene variant	59	41	51
Total	**2751**	**1417**	**1658**

Summary	EMT-6/CDDP	EMT-6/CTX	EMT-6/CTX2
SNPs	2292	1014	1234
Indels	459	403	424
Total	**2751**	**1417**	**1658**

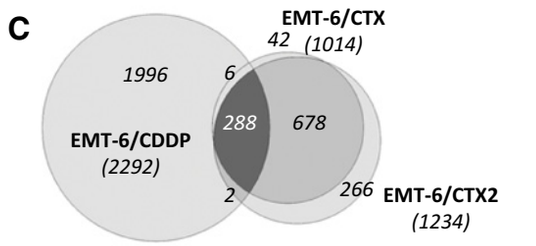

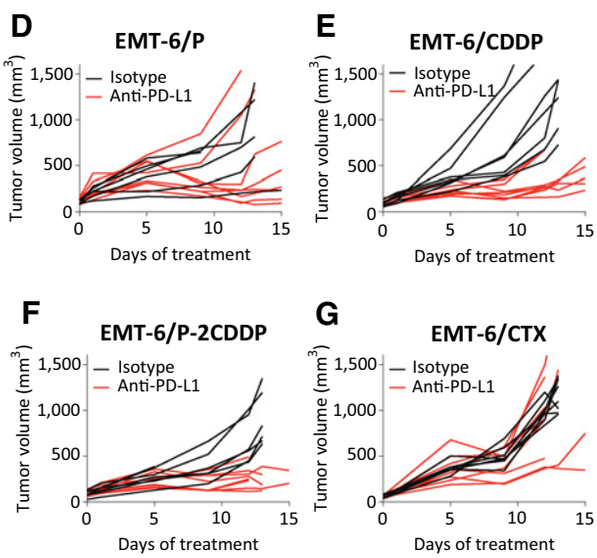

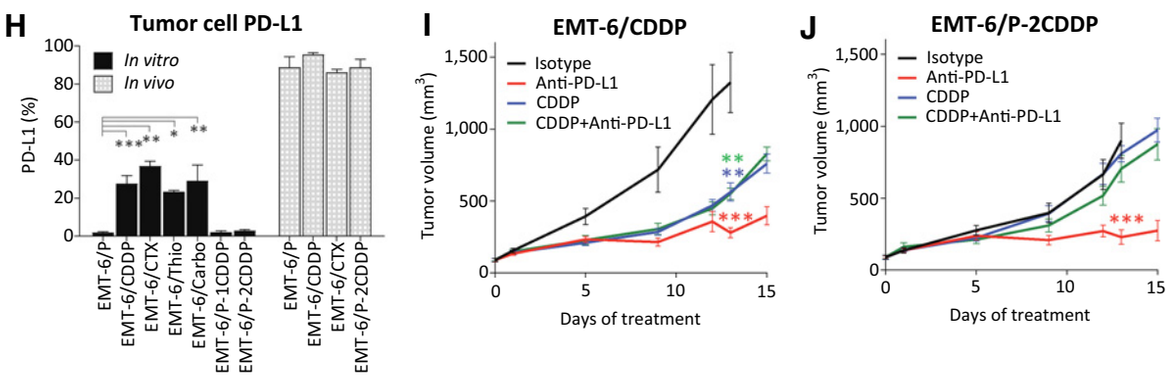

chemotherapy; however, the addition of cisplatin was detrimental and blocked the efficacy of anti-PD-L1 (Fig. 6I and J).

In summary, *in vivo* high dose repetitive cisplatin or cyclophosphamide chemotherapy exposure induced a high number of somatic mutations in tumor cells, which for cisplatin influenced response to PD-L1 blockade. Chemically mutagenized tumor variants revealed linkages between tumor mutational load, immunogenicity, and changes in the immune infiltrate, which on rare occasions corresponded with improved responses to PD-L1 blockade.

Discussion

Summary

Results obtained using mouse models have historically overpredicted clinical benefit to cancer therapy especially when treating primary tumours (40), with a possible exception being immune checkpoint inhibitors. Current models may be underestimating benefit in certain patient subgroups (3, 15, 16). Concerns remain as to the relevance of syngeneic mouse tumors to human malignancies (20). Chemotherapy-treated or refractory tumors in patient populations are rarely (if at all) modeled in mice, yet they comprise a substantial fraction of those patients treated with checkpoint inhibitors. Here we demonstrated that poorly immunogenic mouse tumor cell lines can be rendered more immunogenic by chemical mutagenesis-induced mutational load increase, and in some cases, this translates to heightened tumor responsiveness to PD-L1 inhibition. Chronic chemotherapy exposure of tumor cells with cisplatin or cyclophosphamide *in vivo* also induced high numbers of mutations and preliminary evidence suggests a PD-L1–sensitizing effect by cisplatin exposure. A minority of mutagenized mouse tumor variants therefore recapitulate a general clinical trend where tumors with a higher mutational load tend to respond more favorably to checkpoint inhibitors (4–9).

Relationship between tumor mutational load and checkpoint inhibitor response

As far as we are aware, our data are among the first (see reference 25) to directly demonstrate a relationship between mutational load and checkpoint inhibitor sensitivity in mice. However, a surprising result was that mutational load increase did not correspond with improved immune checkpoint inhibitor responses for 3 of 5 of the tumor cell lines tested, and complete tumor regressions remained rare in responding tumors. An abstract in press describes UV radiation exposure as another strategy to increase the mutational load of BRAFV600E-driven mouse melanoma; however, this also failed to incur sensitivity to PD-1 blockade (41). Mutational burden analysis of a wide range of mouse tumors found no significant correlation with PD-1, PD-L1, or CTLA-4 blockade activity (24, 42). A statistically significant relationship was reported only with dual CTLA-4/PD-1 inhibition (24). Thus, our findings with monotherapy PD-L1 antibody treatment are in line with other reports.

Collectively, these partially negative preclinical data may be clinically relevant. Outliers have been observed in melanoma patients treated with anti-CTLA-4 and NSCLC patients treated with anti-PD-1 antibodies, where the range of mutational or neoantigen load of pretreatment tumors overlap between responder and nonresponder groups (4, 6, 7, 43). Mutational load was predictive of overall survival but was not significantly associated with tumor response to checkpoint inhibitor therapy (43). Thus, a high mutational load does not predict response and a low mutational load does not necessarily predict resistance.

There are several potential genetic explanations for this discordance. First, a high mutational load increases the chances of generating neoantigens but it does not guarantee it (44). For example, of 1,290 amino acid changes, only three validated immunogenic MHC-I–bound neoepitopes existed in MC38 cells (19). In addition to a minor increase of mutations, a lack of immunogenic neoepitopes may explain the anti-PD-L1 unresponsiveness of mutagenized RENCA; however, this is unlikely to explain the unresponsiveness of in highly immunogenic CT26 and MC38 variants. Second, genetic alterations in DNA repair pathways may be more important for immune checkpoint responses than overall mutational burden due to the progressive and dynamic nature of this mutational phenotype and fluctuation of neoantigens over time (9, 25, 43). This concept has been supported by a recent elegant study using genome editing to inactivate MMR gene MutL homolog 1 (*MLH1*) in mouse tumor cells (25). Examples of DNA repair pathway mutations were identified in PD-L1 antibody–responsive EMT-6/P-MNNG+EMS+, but none in RENCA-MNNG+EMS+ variant. Finally, clonal rather than subclonal neoantigens have been proposed to be critical for generating reactive T cells against all tumor cells and eliciting treatment responses (45). Subclonal neoantigens could have played a role in our studies as mutagenized variants consisted of a mixture of clones. Future work will characterize the T-cell–reactive neoantigens that confer antitumor immunity in mutagenized tumors.

Nongenetic determinants of anti-PD-L1 treatment responses

We explored various predictive biomarkers of checkpoint inhibitor therapeutic response using mutagenized and parental tumor variants (38). Similar to results in melanoma (46), baseline levels, and changes in $CD8^+$ T-cell frequency generally correlated with tumor immunogenicity and anti-PD-L1 activity in EMT-6/P, B16F1, and RENCA variants. This relationship was most apparent

Figure 6.

Mutagenic effects of long-term repeated chemotherapy exposure and impact on PD-L1 blockade activity. **A,** Generation of several EMT-6 variants by exposure of tumor-bearing mice or tumor cells to repeated long-term administration of cisplatin (CDDP) or cyclophosphamide (CTX) chemotherapy. †, EMT-6/P, EMT-6/CDDP, and EMT-6/CTX were previously derived by repeated tumor passaging in new hosts following transient lethal doses of chemotherapy (31). ‡, EMT-6/P-2CDDP was previously derived by gradually increasing concentrations of cisplatin *in vitro* (32). δ, EMT-6/CTX2 were rederived from EMT-6/CTX tumors following two cycles of *in vivo* MTD CTX. **B,** Summary of types of somatic mutations detected by exome sequencing of EMT-6/P chemotherapy-exposed variant cells. Mutations listed are those acquired relative to parental control cells. **C,** Total (in brackets) and shared quantity of acquired SNPs in EMT-6/CDDP, EMT-6/CTX and EMT-6/CTX2 variants. **D,** Volumes of EMT-6/P tumors treated with isotype control or anti-PD-L1 antibody 3 × 100 μg i.p. on days 0, 3, and 7. Treatment of EMT-6/CDDP (**E**), EMT-6/P-2CDDP (**F**), and EMT-6/CTX (**G**) tumors ($n = 7$–8). **H,** EMT-6 chemotherapy-exposed variant expression of PD-L1 with significantly higher *in vitro* expression in variants derived *in vivo* and no differences in expression *in vivo* (on $CD45^-$ tumor cells). **I** and **J,** Mean tumor volumes of control, anti-PD-L1, MTD cisplatin (6 mg/kg i.p. days 1, 3, and 5) and combination therapy ($n = 7$–8) treated mice. Statistically significant differences in tumor volume on day 13 are shown relative to Control group. $P > 0.05$ between cisplatin and cisplatin + PD-L1 treatment groups. Note that control and anti-PD-L1 treated mice are those shown in **E** and **F**. *, $P < 0.05$; **, $P < 0.01$; ***, $P < 0.001$. Error bars, SEM.

in well-infiltrated and therapy-responsive mutagenized EMT-6/P tumors. On the other extreme, nonimmunogenic mutagenized RENCA variants appeared "immunologically ignorant" (38) predominated by immunosuppressive cell types.

Tumor immunogenicity is another factor associated with immune checkpoint therapy response in patients (15) and in mouse models (17, 21, 47). Some mutagenized tumor variants did not apparently become immunogenic which was to be expected as chemical mutagen treatment causes variable rates of nontumorigenic (tum-) clones in a cell line–dependent manner (29). Yet, immunogenicity was not sufficient for increasing anti-PD-L1 treatment responses as best exemplified by MC38-MNNG+EMS+ and CT26-MNNG+EMS+, highly immunogenic variants. These variants may be useful to investigate mechanisms of innate resistance to immunotherapy such as neoantigen loss or MHC-I downregulation (48, 49). Finally, we found no clear correlation between PD-(L)1 expression and treatment response in mutagenized tumors (39). The implications of upregulated PD-L1 on *in vivo* passaged and chemotherapy-exposed tumor cells are currently unclear.

Implications of chemotherapy as a mutagenic agent

An important implication of our work is that some chemotherapy agents may influence outcomes with immune checkpoint inhibitors. In accord with the strong impact on mutations in EMT-6/CDDP, cisplatin was found to be the most mutagenic of eight common chemotherapy agents, among them cyclophosphamide (11). A mutational load increase is also probable of EMT-6/P-2CDDP variant, which also has downregulated mismatch repair enzymes MLH1 and PMS2 (32). Exposure to mutagenic chemotherapy regimens may therefore increase tumor neoantigens and render unresponsive immunologically "cold" tumors more sensitive to checkpoint blockade (50). There are some clinical data to support this idea. The PD-L1 antibody atezolizumab demonstrated activity in urothelial carcinoma patients who had progressed following treatment with platinum-based chemotherapy. Mutational load was an independent predictor of response (51). A similar relationship with mutational burden was reported in a platinum-resistant ovarian cancer patient who experienced prolonged treatment benefit from the PD-L1 antibody avelumab (52).

Optimal strategies to incorporate chemotherapy with checkpoint inhibitors need to be defined. Two methods include sequencing conventional MTD chemotherapy with a checkpoint inhibitor or administering the drugs concurrently. We and others (53) have observed concurrent treatment to be ineffective preclinically. Although chemotherapy may induce neoantigens, such antigens may be subclonal that are linked with poor checkpoint inhibitor response (45). Alternatively, low-dose metronomic chemotherapy with agents such as cyclophosphamide, which can stimulate $CD8^+$ T-cell effector activity (54, 55), may potentially provide an ideal partner with immune checkpoint therapy. Regardless, the above strategies will likely be unsuccessful in patients with high levels of chemotherapy-induced immunosuppression. Finally, another strategy is to use chemotherapy agents which inactivate/suppress DNA mismatch repair enzymes, e.g. temozolamide, as recently reported by Germano et al. (25).

Limitations

A key limitation of our study is that our findings were primarily correlative, and we did not prove that the increased anti-PD-L1 responsiveness of the EMT-6/P mutagenized variants and impaired growth rates of other lines is a direct cause of an increase in the mutational or neoantigen load. Nonetheless, we believe that the differential responsiveness in some (but not all) cell lines are interesting and potentially important results, particularly from the perspective of preclinical experimental studies. This study is a first step in the characterization of these variants and exploring how they might be applied as experimental tools. Thus, areas for future work include evaluating the T-cell responses to induced neoantigens, uncovering whether responses are $CD4^+$ or $CD8^+$ T-cell–specific, or evaluating differential responses of another checkpoint inhibitor. For example, antibodies against CTLA-4 rather than PD-(L)1 would likely yield distinct antitumor responses due to the involvement of CTLA-4 in downregulating initiation of adaptive immunity (1). A second major limitation of our study stems from the pooling of mutagenized clones. On one hand, this approach mimics the genetic heterogeneity of human tumors, but on the other, it may dilute the overall impact of immunogenic clones and confound interpreting mutational data. Evolving dominance of certain clones in culture may cause divergence of different passages of cells. Evaluating multiple clones *in vivo* would be resource intensive, but potentially valuable if growth-proficient immunogenic variants are generated.

Conclusions

Chemical mutagenesis is a known method to enhance the immunogenicity of cell lines (27, 29) and we propose that this methodology could also be used to improve the utility of previously immune therapy refractory models, such as B16 melanoma, for certain immunotherapy studies. The reduced growth rates of certain mutagenized variants may potentially minimize overload on the immune system, which is problematic for therapy studies with rapidly progressing mouse tumor models. Our approach now enables undertaking experiments that directly compare paired mutagenized and parental lines, which could also be undertaken in models of metastatic disease. This experimental tool could aid in evaluating the impact of therapy combinations on different inflammatory subsets of the same tumor or identifying mechanisms of immunotherapy resistance. In conclusion, increasing the mutational load of mouse tumor cell lines by chemical mutagens and certain chemotherapy agents was associated with enhanced PD-L1 blockade sensitivity of only a minority of poorly immunogenic mouse tumor cell lines. Our data further highlights the complexity of factors involved in immunotherapy responding and resistant tumors.

Disclosure of Potential Conflicts of Interest

No potential conflicts of interest were disclosed.

Authors' Contributions

Conception and design: E.A. Kuczynski, J. Krueger, R.S. Kerbel
Development of methodology: E.A. Kuczynski, J. Krueger, P.M. Krzyzanowski
Acquisition of data (provided animals, acquired and managed patients, provided facilities, etc.): E.A. Kuczynski, J. Krueger, A. Chow, J.K. Miller, P.M. Krzyzanowski
Analysis and interpretation of data (e.g., statistical analysis, biostatistics, computational analysis): E.A. Kuczynski, J. Krueger, Y. Sundaravadanam, P.M. Krzyzanowski
Writing, review, and/or revision of the manuscript: E.A. Kuczynski, J. Krueger, A. Chow, P. Xu, J.K. Miller, P.M. Krzyzanowski, R.S. Kerbel

Administrative, technical, or material support (i.e., reporting or organizing data, constructing databases): E.A. Kuczynski, J. Krueger, A. Chow, P. Xu, S. Man, J.K. Miller
Study supervision: A. Chow, R.S. Kerbel

Acknowledgments

This work was mainly funded by research grants (awarded to R.S. Kerbel) from the Canadian Breast Cancer Foundation (CBCF), and the Canadian Institutes of Health Research (CIHR; grant number PJT-148542). We thank Cassandra Cheng for excellent secretarial assistance.

The costs of publication of this article were defrayed in part by the payment of page charges. This article must therefore be hereby marked *advertisement* in accordance with 18 U.S.C. Section 1734 solely to indicate this fact.

Received November 6, 2017; revised December 4, 2017; accepted February 1, 2018; published first February 26, 2018.

References

1. Pardoll DM. The blockade of immune checkpoints in cancer immunotherapy. Nat Rev Cancer 2012;12:252–64.
2. Alexandrov LB, Nik-Zainal S, Wedge DC, Aparicio SA, Behjati S, Biankin AV, et al. Signatures of mutational processes in human cancer. Nature 2013;500:415–21.
3. Topalian SL, Taube JM, Anders RA, Pardoll DM. Mechanism-driven biomarkers to guide immune checkpoint blockade in cancer therapy. Nat Rev Cancer 2016;16:275–87.
4. Rizvi NA, Hellmann MD, Snyder A, Kvistborg P, Makarov V, Havel JJ, et al. Cancer immunology. Mutational landscape determines sensitivity to PD-1 blockade in non-small cell lung cancer. Science 2015;348:124–8.
5. Johnson DB, Frampton GM, Rioth MJ, Yusko E, Xu Y, Guo X, et al. Targeted next generation sequencing identifies markers of response to PD-1 Blockade. Cancer Immunol Res 2016;4:959–67.
6. Snyder A, Makarov V, Merghoub T, Yuan J, Zaretsky JM, Desrichard A, et al. Genetic basis for clinical response to CTLA-4 blockade in melanoma. N Engl J Med 2014;371:2189–99.
7. Van Allen EM, Miao D, Schilling B, Shukla SA, Blank C, Zimmer L, et al. Genomic correlates of response to CTLA-4 blockade in metastatic melanoma. Science 2015;350:207–11.
8. Bouffet E, Larouche V, Campbell BB, Merico D, de Borja R, Aronson M, et al. Immune checkpoint inhibition for hypermutant glioblastoma multiforme resulting from germline biallelic mismatch repair deficiency. J Clin Oncol 2016;34:2206–11.
9. Le DT, Uram JN, Wang H, Bartlett BR, Kemberling H, Eyring AD, et al. PD-1 blockade in tumors with mismatch-repair deficiency. N Engl J Med 2015;372:2509–20.
10. U.S. Food and Drug Administration. FDA approves first cancer treatment for any solid tumor with a specific genetic feature; 2017. Available from: https://www.fda.gov/newsevents/newsroom/pressannouncements/ucm560167.htm.
11. Szikriszt B, Poti A, Pipek O, Krzystanek M, Kanu N, Molnar J, et al. A comprehensive survey of the mutagenic impact of common cancer cytotoxics. Genome Biol 2016;17:99.
12. Dempsey JL, Seshadri RS, Morley AA. Increased mutation frequency following treatment with cancer chemotherapy. Cancer Res 1985;45:2873–7.
13. Brahmer J, Reckamp KL, Baas P, Crino L, Eberhardt WE, Poddubskaya E, et al. Nivolumab versus docetaxel in advanced squamous-cell non-small-cell lung cancer. N Engl J Med 2015;373:123–35.
14. Ansell SM, Lesokhin AM, Borrello I, Halwani A, Scott EC, Gutierrez M, et al. PD-1 blockade with nivolumab in relapsed or refractory Hodgkin's lymphoma. N Engl J Med 2015;372:311–9.
15. Grosso JF, Jure-Kunkel MN. CTLA-4 blockade in tumor models: an overview of preclinical and translational research. Cancer Immunity 2013;13:5.
16. Herbst RS, Soria JC, Kowanetz M, Fine GD, Hamid O, Gordon MS, et al. Predictive correlates of response to the anti-PD-L1 antibody MPDL3280A in cancer patients. Nature 2014;515:563–7.
17. Lechner MG, Karimi SS, Barry-Holson K, Angell TE, Murphy KA, Church CH, et al. Immunogenicity of murine solid tumor models as a defining feature of in vivo behavior and response to immunotherapy. J Immunol 2013;36:477–89.
18. Vesely MD, Kershaw MH, Schreiber RD, Smyth MJ. Natural innate and adaptive immunity to cancer. Annu Rev Immunol 2011;29:235–71.
19. Yadav M, Jhunjhunwala S, Phung QT, Lupardus P, Tanguay J, Bumbaca S, et al. Predicting immunogenic tumour mutations by combining mass spectrometry and exome sequencing. Nature 2014;515:572–6.
20. Gould SE, Junttila MR, de Sauvage FJ. Translational value of mouse models in oncology drug development. Nat Med 2015;21:431–9.
21. Mosely SI, Prime JE, Sainson RC, Koopmann JO, Wang DY, Greenawalt DM, et al. Rational selection of syngeneic preclinical tumor models for immunotherapeutic drug discovery. Cancer Immunol Res 2017;5:29–41.
22. Barnes S, Miliani de Marval P, Hauser J, Brainard T, Small D, Synnott AJ, et al. Abstract 3362: systematic evaluation of immune checkpoint inhibitors. Cancer Res 2015;75:3362-.
23. Gubin MM, Zhang X, Schuster H, Caron E, Ward JP, Noguchi T, et al. Checkpoint blockade cancer immunotherapy targets tumour-specific mutant antigens. Nature 2014;515:577–81.
24. Zeitouni B, Tschuch C, Davis JM, Peille A-L, Raeva Y, Landesfeind M, et al. Abstract 1840: Whole-exome somatic mutation analysis of mouse cancer models and implications for preclinical immunomodulatory drug development. Cancer Res 2017;77:1840.
25. Germano G, Lamba S, Rospo G, Barault L, Magri A, Maione F, et al. Inactivation of DNA repair triggers neoantigen generation and impairs tumour growth. Nature 2017;552:116–20.
26. Foster PL. In vivo mutagenesis. Methods Enzymol 1991;204:114–25.
27. Boon T, Kellermann O. Rejection by syngeneic mice of cell variants obtained by mutagenesis of a malignant teratocarcinoma cell line. Proc Natl Acad Sci U S A 1977;74:272–5.
28. Van Pel A, Georlette M, Boon T. Tumor cell variants obtained by mutagenesis of a Lewis lung carcinoma cell line: immune rejection by syngeneic mice. Proc Natl Acad Sci U S A 1979;76:5282–5.
29. Frost P, Kerbel RS, Bauer E, Tartamella-Biondo R, Cefalu W. Mutagen treatment as a means for selecting immunogenic variants from otherwise poorly immunogenic malignant murine tumors. Cancer Res 1983;43:125–32.
30. Boon T, Van Pel A. Teratocarcinoma cell variants rejected by syngeneic mice: protection of mice immunized with these variants against other variants and against the original malignant cell line. Proc Natl Acad Sci U S A 1978;75:1519–23.
31. Teicher BA, Herman TS, Holden SA, Wang YY, Pfeffer MR, Crawford JW, et al. Tumor resistance to alkylating agents conferred by mechanisms operative only in vivo. Science 1990;247:1457–61.
32. Francia G, Green SK, Bocci G, Man S, Emmenegger U, Ebos JM, et al. Down-regulation of DNA mismatch repair proteins in human and murine tumor spheroids: implications for multicellular resistance to alkylating agents. Mol Cancer Ther 2005;4:1484–94.
33. Cibulskis K, Lawrence MS, Carter SL, Sivachenko A, Jaffe D, Sougnez C, et al. Sensitive detection of somatic point mutations in impure and heterogeneous cancer samples. Nat Biotechnol 2013;31:213–9.
34. Saunders CT, Wong WS, Swamy S, Becq J, Murray LJ, Cheetham RK. Strelka: accurate somatic small-variant calling from sequenced tumor-normal sample pairs. Bioinformatics 2012;28:1811–7.
35. Schumacher TN, Schreiber RD. Neoantigens in cancer immunotherapy. Science 2015;348:69–74.
36. Giannakis M, Mu XJ, Shukla SA, Qian ZR, Cohen O, Nishihara R, et al. Genomic correlates of immune-cell infiltrates in colorectal carcinoma. Cell Rep 2016;17:1206.
37. Angelova M, Charoentong P, Hackl H, Fischer ML, Snajder R, Krogsdam AM, et al. Characterization of the immunophenotypes and antigenomes of colorectal cancers reveals distinct tumor escape mechanisms and novel targets for immunotherapy. Genome Biol 2015;16:64.
38. Hegde PS, Karanikas V, Evers S. The where, the when, and the how of immune monitoring for cancer immunotherapies in the era of checkpoint inhibition. Clin Cancer Res 2016;22:1865–74.
39. Ribas A, Hu-Lieskovan S. What does PD-L1 positive or negative mean? J Exp Med 2016;213:2835–40.

40. Francia G, Cruz-Munoz W, Man S, Xu P, Kerbel RS. Mouse models of advanced spontaneous metastasis for experimental therapeutics. Nat Rev Cancer 2011;11:135–41.
41. Galvani E, Hogan K, Gremel G, Viros A, Mandal AK, Smith M, et al. Abstract 3207: Influence of tumor mutation burden on response to anti-PD-1 treatment in murine models of melanoma. Cancer Res 2016;76:3207.
42. Lagrange A, Boidot R, Hillairet de Boisferon M, Duchamp O, Mirjolet J-F, Ghiringhelli F. Abstract 3226: Efficacy of PD-1 - PD-L1 pathway disruptors in syngeneic models. Cancer Res 2016;76:3226-.
43. Hugo W, Zaretsky JM, Sun L, Song C, Moreno BH, Hu-Lieskovan S, et al. Genomic and transcriptomic features of response to anti-PD-1 therapy in metastatic melanoma. Cell 2016;165:35–44.
44. Gubin MM, Schreiber RD. CANCER. The odds of immunotherapy success. Science 2015;350:158–9.
45. McGranahan N, Furness AJ, Rosenthal R, Ramskov S, Lyngaa R, Saini SK, et al. Clonal neoantigens elicit T cell immunoreactivity and sensitivity to immune checkpoint blockade. Science 2016;351:1463–9.
46. Tumeh PC, Harview CL, Yearley JH, Shintaku IP, Taylor EJ, Robert L, et al. PD-1 blockade induces responses by inhibiting adaptive immune resistance. Nature 2014;515:568–71.
47. Leach DR, Krummel MF, Allison JP. Enhancement of antitumor immunity by CTLA-4 blockade. Science 1996;271:1734–6.
48. Matsushita H, Sato Y, Karasaki T, Nakagawa T, Kume H, Ogawa S, et al. Neoantigen load, antigen presentation machinery, and immune signatures determine prognosis in clear cell renal cell carcinoma. Cancer Immunol Res 2016;4:463–71.
49. Donia M, Harbst K, Van Buuren M, Kvistborg P, Lindberg MF, Andersen R, et al. Acquired immune resistance follows complete tumor regression without loss of target antigens or IFN-γ signaling. Cancer Res 2017;77:4562—6.
50. Greil R, Hutterer E, Hartmann TN, Pleyer L. Reactivation of dormant antitumor immunity - a clinical perspective of therapeutic immune checkpoint modulation. Cell Commun Signal 2017;15:5.
51. Rosenberg JE, Hoffman-Censits J, Powles T, van der Heijden MS, Balar AV, Necchi A, et al. Atezolizumab in patients with locally advanced and metastatic urothelial carcinoma who have progressed following treatment with platinum-based chemotherapy: a single-arm, multicentre, phase 2 trial. Lancet 2016;387:1909–20.
52. Morse CB, Elvin JA, Gay LM, Liao JB. Elevated tumor mutational burden and prolonged clinical response to anti-PD-L1 antibody in platinum-resistant recurrent ovarian cancer. Gynecol Oncol Rep 2017;21:78–80.
53. Parra K, Valenzuela P, Lerma N, Gallegos A, Reza LC, Rodriguez G, et al. Impact of CTLA-4 blockade in conjunction with metronomic chemotherapy on preclinical breast cancer growth. Br J Cancer 2017;116:324–34.
54. Wu J, Waxman DJ. Metronomic cyclophosphamide eradicates large implanted GL261 gliomas by activating antitumor Cd8+ T-cell responses and immune memory. Oncoimmunology 2015;4:e1005521.
55. Ghiringhelli F, Menard C, Puig PE, Ladoire S, Roux S, Martin F, et al. Metronomic cyclophosphamide regimen selectively depletes CD4+CD25+ regulatory T cells and restores T and NK effector functions in end stage cancer patients. Cancer Immunol Immunother 2007;56:641–8.